5-20-2019

Analysis of Septum Defects in Arabidopsis Organ Boundary Mutants

Katherine T. Anderson
University of Mississippi

Analysis of Septum Defects in *Arabidopsis* Organ Boundary Mutants

By: Katherine Taylor Anderson

A thesis submitted to the faculty of The University of Mississippi in partial fulfillment of the requirements of the Sally McDonnell Barksdale Honors College.

Oxford
May 2019

Approved by:

_____
Advisor: Dr. Sarah Liljegren

_____
Reader: Dr. Bradley Jones

_____
Reader: Dr. Susan Pedigo

ACKNOWLEDGEMENTS

I would first like to thank Dr. Sarah Liljegren for allowing me to join her lab and working with me to develop this project. Without Dr. Liljegren's constant positive attitude and words of affirmation, this thesis would not have been possible. I am immensely grateful for the countless hours Dr. Liljegren has spent teaching me and editing my thesis. She has fostered a supportive lab environment, and I was never once afraid to ask a question.

This project would not have succeeded without the help of our lab assistant, Kate Childers. Kate trained me in the lab and contributed to this project by caring for the plants and helping me complete the genotyping process. Kate also has edited my thesis numerous times and provided valuable advice. Aside from the work she performed in the lab, Kate was a source of encouragement throughout this entire process, and I am thankful that she was there in times of stress.

I also want to thank Jack Mason, Alex Kissel, John Salvemini, Kayla Woodson, and Landon Goodreau for assisting me and contributing to a positive environment in the lab. They have been patient and helpful as I worked to complete this thesis.

Lastly, I would like to thank the Sally McDonnell Barksdale Honors College for providing me with this opportunity and helping me along the way. I am thankful for this entire experience as I have gained knowledge that will benefit me in my future endeavors.

This research was supported by an NSF grant (IOS- 1453733) to SL.

ABSTRACT

KATHERINE TAYLOR ANDERSON: Analysis of Septum Defects in *Arabidopsis* Organ Boundary Mutants (Under the direction of Dr. Sarah Liljegren)

Arabidopsis thaliana, a model plant species, has been heavily studied to determine the genetic contributions that lead to gynoecium development. The *Arabidopsis* fruit is created from two carpels that form a gynoecium, which contains the stigma, style, and ovary. The ovary is divided into two sub-compartments by a septum, and the ovules develop within the ovary. The fruit's purpose is to protect, nurture, and eventually disperse the mature ovules, or seeds, and if the septum does not fuse properly, the plant's fertility will be impacted. *SHOOT MERISTEMLESS (STM)* and *ARABIDOPSIS THALIANA HOMEOBOX GENE1 (ATH1)* are two genes that are known to be involved in fruit development, specifically meristem maintenance and organ boundary specification. Plants with mutations in both *STM* and *ATH1* produce fruit with multiple developmental defects.

To investigate the effects of *stm* and *ath1* mutations on septum development, I analyzed the septa of *stm, ath1, stm/+ ath1, and stm ath1* fruit in comparison to wild-type fruit. Because STM maintains the stem cell population in flower meristems and induces the biosynthesis of cytokinin in the carpel margin meristem (which includes the septum), I hypothesized that *stm* mutant fruit would display moderate septum defects. Also, because previous studies have shown that ATH1 and STM act redundantly in promoting fruit development, I hypothesized that the *stm ath1* double mutant fruit would have enhanced septum defects compared to the *stm* single mutant. To evaluate the septum

fusion defects, I measured the amount of septum surface area missing in relation to the total potential septum surface area for each fruit. This study revealed that 50 of the 51 *stm* single mutant fruit had septa fusion defects, while none of the *ath1-5* fruit had abnormal septa. In addition, I found that the fusion defects present in the *stm ath1-5* double mutant were not significantly enhanced relative to the *stm* single mutant. These results suggest that *STM* alone plays a critical role in fusion of the septum during fruit development.

TABLE OF CONTENTS

LIST OF FIGURES AND TABLES

LIST OF ABBREVIATIONS

Arabidopsis: *Arabidopsis thaliana*

ATH1: *ARABIDOPSIS THALIANA HOMEOBOX GENE 1*

ath1: *ATH1* mutant

bHLH: basic helix-loop-helix

bp: base pair

CMM: carpel margin meristem

CUC1: *CUP-SHAPED COTELYDON 1*

cuc1: *CUP-SHAPED COTELYDON 1* mutant

CUC2: *CUP-SHAPED COTELYDON 2*

cuc2: *CUP-SHAPED COTELYDON 2* mutant

ddH_2O: deionized water

DNA: deoxyribonucleic acid

KNOX: class I KNOTTED-LIKE HOMEOBOX

Ler: Landsberg *erecta*

NLS: nuclear localization signal

PCR: polymerase chain reaction

RNAi: RNA interference

SAM: shoot apical meristem

SEM: scanning electron micrograph

SPT: *SPATULA*

spt: *SPATULA* mutant

STM: *SHOOT MERISTEMLESS*

stm: *STM* mutant

TF: transcription factor

WT: wildtype

INTRODUCTION

Arabidopsis thaliana is often used as a model organism in plant research because of its short life cycle, self-pollinating flowers, and accessible growth conditions. Furthermore, *Arabidopsis* has a diploid genome consisting of only five chromosomes, and was the first plant to have its genome sequenced (Meinke et al. 1998; The *Arabidopsis* Genome Initiative, 2000). These features have allowed for in depth studies of the molecular mechanisms of gynoecium development in a flowering plant (reviewed in Arnaud and Pautot, 2014). The gynoecium is the female floral organ containing the stigma, style, and ovary, which protects the ovules (**Figure 1A**).

The shoot apical meristem (SAM), a group of undifferentiated, rapidly dividing cells at the tip of the shoot, gives rise to nearly all of the above-ground organs (Takano et al., 2010). The SAM is responsible for the generation of stems, leaves, and floral organs while also maintaining a group of pluripotent (capable of giving rise to many different cell types) stem cells in the center (Aida et al., 1999). Flowers develop from lateral meristems, which are produced by the SAM (Steeves and Sussex, 1989). The peripheral regions of the floral meristem give rise to the floral organ primordia which create the fruit.

The central dome of floral meristem cells gives rise to the gynoecial primordium. This primordium arises as an oval ring of cells, which continues to proliferate into a tube-like structure (Larsson et al., 2013). Even at early stages of development, the medial and lateral domains of the gynoecium can be distinguished. The medial domain gives rise to

the medial ridges that proliferate inward (**Figure 1C**). These cells in the ridges eventually create the ovules, septum, and transmitting tract (Larsson et al., 2013). The two septal primordia arise at the boundaries between the two carpel primordia and form the septum when they proliferate inwards and fuse together (Ishida et al., 2000).

The stigmatic tissue, located at the top of the mature gynoecium, is where pollen grains germinate and subsequently grow down the transmitting tract, which is located at the center of the septum (**Figure 1A**). Since the transmitting tract is required for the growth of pollen tubes toward the ovules, it is essential for fertilization. Therefore, if the septum is not correctly formed, fertilization will be hindered.

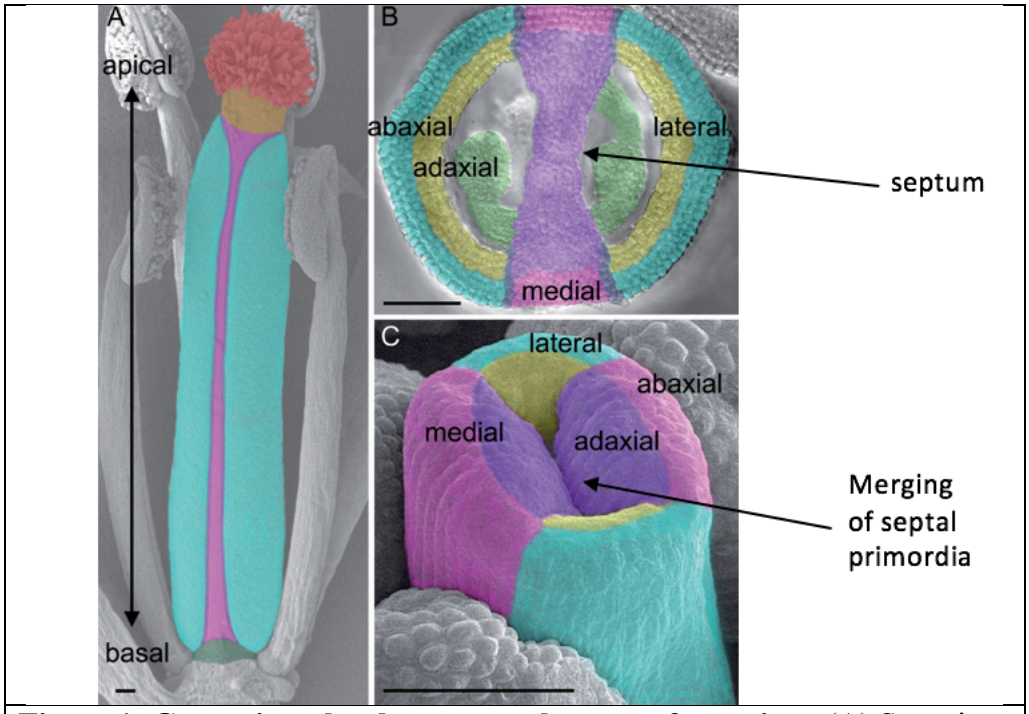

Figure 1: Gynoecium development and septum formation. (A) Scanning electron micrograph of a mature gynoecium. (B) Cross section of gynoecium showing the septal tissue in purple. (C) Developing gynoecium prior to septal fusion. (Images from Larsson et al., 2013)

After fertilization, the pistil elongates into a fruit consisting of multiple cell types that serve to protect the developing seeds, as well as contribute to seed dispersal at the

time of maturation (Liljegren et al. 2004). The *Arabidopsis* fruit is composed of two valves separated by a medial ridge called the replum and the internal septum (**Figure 2B**). The septum separates the two rows of ovules inside the enclosed fruit. The thin margins between the valves and the replum consist of specialized cells that become lignified to promote the dehiscence of the fruit. Dehiscence, or pod-shatter, is the process by which the two valves detach from the fruit to release the seeds, and each cell type shown in **Figure 2** contributes to this pod-shatter mechanism. The cell walls of the valve and margin layers begin to stiffen through the cellular process of lignification, which, when paired with the shrinkage of the remaining valve cells creates tension within the fruit, causing it to dehisce or "shatter" (Liljegren et al. 2004). Geneticists have extensively studied various genes to learn more about their role in fruit cell-type differentiation and fruit growth and development.

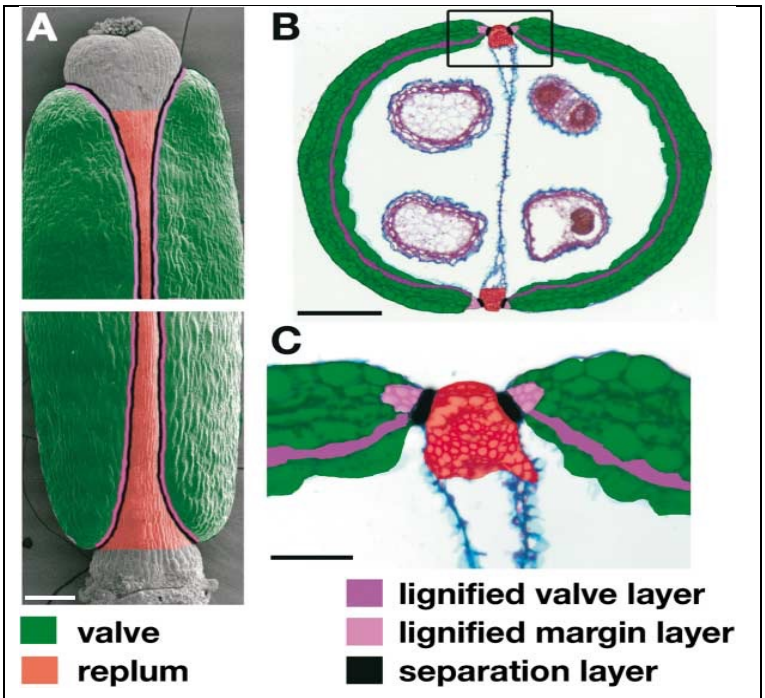

Figure 2: Differentiated Cell Types in *Arabidopsis* fruit. A) Scanning electron micrograph (SEM) of a wild type fruit, colored to specify fruit regions. B) Cross section of wild type fruit including ovules, septum, and distinct cell types. C) Enlarged image of the valve margin and separation layer (Photo credit: Liljegren et al, 2004)

One of the genes utilized in this study is *SHOOT MERISTEMLESS (STM)*, which encodes a KNOTTED-LIKE homeodomain transcription factor. *STM* plays a fundamental role in maintaining pools of undifferentiated stem cells in both the shoot apical meristem (SAM), a region of actively dividing cells at the uppermost tip of the growing plant, and the floral meristem, which gives rise to the flower (Scofield et al. 2014). In loss-of-function *stm* mutants, cells in the central zone of the shoot meristem are lost, which results in termination of the primary shoot meristem at the seedling stage of development (Endrizzi et al. 1996). The cotyledons, two seed leaves within the embryo of an *Arabidopsis* seed, can be partially fused around the reduced shoot meristem of *stm*

seedlings. These results provided the initial evidence that STM is involved in replenishing stem cells in flowering plants and suggested its role in maintaining organ boundaries (Endrizzi et al. 1996).

A novel hypomorphic allele of *STM* has a point mutation that changes a tryptophan (W) at amino acid 343 in the homeodomain region of the STM transcription factor to a premature stop codon (see **Figure 3A**; Liljegren, unpublished results). As this mutation only partially reduces STM function, it has been valuable for further dissecting the roles of STM in fruit development (Childers, 2018) and in specifying organ boundaries (Malone, 2018; Palmer, 2018). This *stm* single mutant typically has reduced fruit length and width compared to wild-type fruit (Childers, 2018), a few less petals and stamens, and some fused stamens (Malone, 2018). Additionally, the organ boundaries between the sepals and floral stem of *stm* single mutants are less distinct (Liljegren, unpublished results).

ARABIDOPSIS THALIANA HOMEOBOX GENE1 (ATH1) encodes a BELL-type homeodomain transcription factor, and is required for formation of boundary regions between the floral organs and the underlying stem (Gomez-Mena and Sablowski, 2008). ATH1 has also been shown to work alongside light-activated genes to repress stem growth during the vegetative phase of the *Arabidopsis* life cycle because when *ATH1* expression was repressed, growth in this region was enhanced. Furthermore, when *ATH1* was constitutively expressed during the flowering stage, the inflorescence stem and floral pedicels stopped growing, which is consistent with the idea that *ATH1* restricts growth in organ boundary regions and in the stem by inhibiting cellular proliferation (Gomez-Mena and Sablowski, 2008).

The *ath1-5* allele used in this study has a splice site error that introduces a premature stop codon in place of the tyrosine (Y) amino acid at position 399; this affects the DNA-binding region of the transcription factor (**Figure 3B**, Liljegren, unpublished results). The phenotype of *ath1-5* flowers resembles those of the *ath1-3* mutants (Malone, 2018; Leary, 2018; Roth, 2018; Palmer, 2018); therefore, both are considered to represent loss-of-function alleles (Gomez-Mena and Sablowski 2008; Liljegren, unpublished results). Fruit with an *ath1-5* single mutation also have reduced length and width with respect to wild-type fruit (Childers, 2018). The *ath1-5* single mutant flowers also display a higher frequency of stamen-stamen fusions than wild-type flowers (Malone, 2018), and like *stm* flowers, have less distinct sepal-floral stem organ boundaries (Liljegren, unpublished results).

Figure 3: Mutations in *STM* and *ATH1* affect the homeodomain regions of the encoded transcription factors. A) At amino acid 343, a tryptophan (W) is replaced by a premature stop codon. B) A splice-site error results in a premature stop codon in place of a tyrosine (Y) at position 399. (Liljegren, unpublished results)

STM does not have a nuclear localization signal (NLS) in its amino acid sequence, and therefore, cannot enter the nucleus on its own (Cole et al. 2006). In order to regulate gene transcription in the nucleus, it dimerizes with four different BELL-type homeodomain transcription factors that have a nuclear localization signals, including

ATH1 (Rutjens et al. 2009). Fruit with mutations in both *stm* and *ath1-5* display more dramatic developmental defects than either *stm* or *ath1-5* single mutant fruit, which indicates some redundancy between the roles of ATH1 and STM during fruit development. *stm ath1-5* flowers display significantly fewer petals and stamens and the majority (ie. 75% in one study) are missing the central pistil (Malone, 2018; Childers, 2018). Childers (2018) found that *stm ath1-5* double mutant fruit produced are significantly shorter and thinner than wild-type, and that some of these fruit appeared to have defects in formation of the valve-replum boundary. While STM and ATH1 are very important in fruit development and differentiation, there are many other genes involved in this process as well.

CUP-SHAPED COTYLEDON1 (CUC1) and *CUP-SHAPED COTYLEDON2 (CUC2)*, a pair of NAC transcription factors, have been shown to play a key role in septum development (Ishida et al., 2000). The *cuc1 cuc2* double mutant produces gynoecia with completely unfused septa (**Figure 4**). Because the *cuc1 cuc2* double mutant fruit showed an absence of septal tissue compared to the partial septa in other single mutants, it is believed that the septal primordia in the double mutant may have arrested before elongation (**Figure 4,** Ishida et al. 2000). When *CUC2* expression was analyzed throughout the Arabidopsis life cycle, it was found at the tips of septal primordia just prior to fusion of the septum (Ishida et al. 2000). The absence of septal tissue in *cuc1 cuc2* mutants and the expression of *CUC2* in the septum near the time of fusion suggest that *CUC1* and *CUC2* play a critical role in septum development.

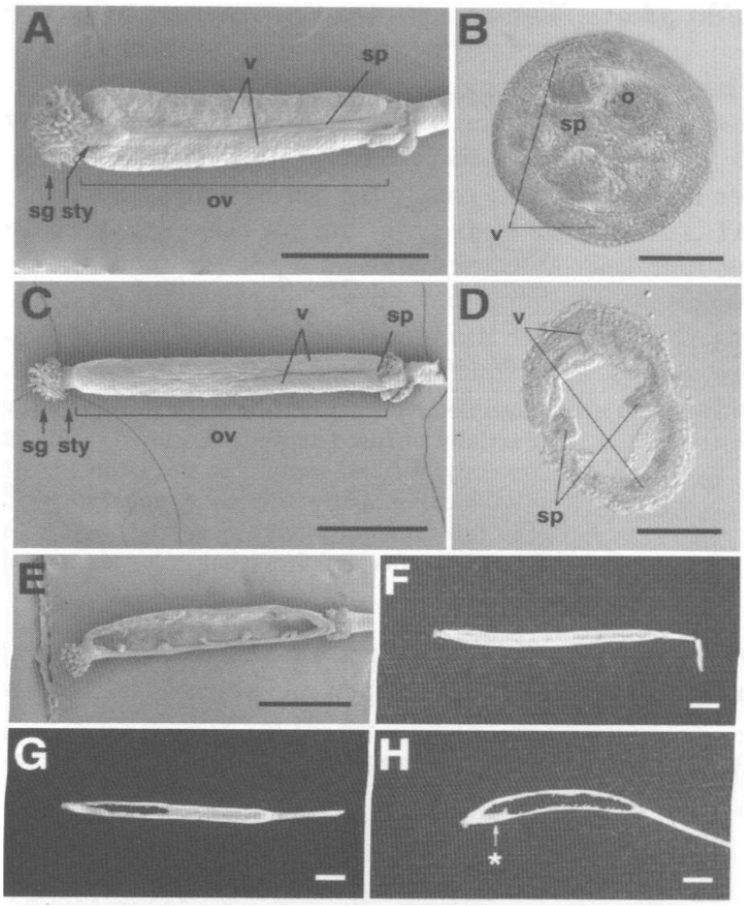

Figure 4: The organ boundary genes CUC1 and CUC2 are required for fusion of the septum. A) SEM of wild-type fruit. B) Cross section of wild-type gynoecium with a fully fused septum. C) SEM of *cuc1 cuc2* double mutant fruit. D) Cross section of *cuc1 cuc2* double mutant fruit showing failure of septum fusion. E) SEM of dissected *cuc1 cuc2* double mutant fruit missing the septum and ovules. (F) to (H): Septa of *cuc1/+ cuc2* plants displaying variable expressivity of the septal fusion defects F) Normal septum. G) A partially unfused septum. H) A severely unfused septum. sg, stigma; sty, style; ov, ovary; v, valve; sp, septum; o, ovule. (Image credit: Ishida et al., 2000)

Another gene, *SPATULA* (*SPT*), works synergistically with *CUC1* and *CUC2* to ensure the proper development of the septum and ovules (Nahar et al., 2012). *SPT* encodes a basic helix-loop-helix (bHLH) transcription factor, and is also well known for its role in promoting fusion of the apical region of the gynoecium near the stigma and

style (Alvarez and Smyth 1999, Alvarez and Smyth 2002). Since the *spt* mutant shows a reduction of medial ridge size, SPT is thought to regulate cell proliferation at these ridges, which would affect both septum and ovule development (Alvarez et al. 1999, Ishida et al. 2000, Takada et al. 2001).

SPT also plays an important role in the medial domain because it enables the cytokinin signaling required for carpel margin meristem (CMM) activity and growth (Reyes-Olalde et al. 2017). Cytokinin is a phytohormone that promotes meristematic activity in cells, and is strongly expressed in the medial rather than the lateral domains of developing gynoecia. Within the CMM, cytokinin promotes proliferation of the cells that will become the septum, replum, placenta, ovules, and transmitting tract (Reyes-Olalde et al. 2017). Furthermore, SPT and cytokinin work together to activate auxin biosynthesis and transport genes, which also contribute to growth in the CMM. Auxin is a plant hormone that promotes the elongation of cells in shoots and regulating plant growth.

STM, as mentioned before, is required for the maintenance of shoot and floral meristems. It activates genes involved in cytokinin biosynthesis such as *ISOPENTENIL TRANSFERASE (IPT)* (Reyes-Olalde et al., 2017). Loss of STM has been found to reduce cytokinin signaling. When STM expression was down-regulated using RNA interference (RNAi), carpels failed to fuse properly and fewer ovules were produced. In weakly affected STM-RNAi flowers, the central carpels failed to properly fuse to form a gynoecium, and in more severely affected STM-RNAi flowers, the gynoecium was completely absent. This study indicates a critical role of STM in the proper formation of carpels and placental tissues. (Scofield et al., 2007)

The aim of this study was to analyze the septum defects of a set of *Arabidopsis* organ boundary mutants. In a pilot study carried out last summer, I examined the septa of several mutant genotypes compared to wild-type, and found that many *stm* single and *stm ath1-5* double mutant fruit contained unfused septa. Based on these results, and on previous studies of the roles of STM and ATH1 in promoting fruit growth (Childers, 2018), my thesis research was designed to test two hypotheses. First, since it is known that STM activates the biosynthesis of cytokinin and thus promotes growth of the central margin meristem (Reyes-Olalde et al. 2017), I hypothesized that *stm* mutants would display moderate to severe septum fusion defects. Second, since STM has previously been shown to promote fruit growth redundantly with ATH1 (Childers, 2018), I hypothesized that *stm ath1-5* double mutants would display severe septum fusion defects or even completely missing septa as was observed in *cuc1 cuc2* double mutant fruit (**Figure 4**; Ishida et al., 2000). To test these hypotheses, I analyzed the septa of *stm, ath1-5, stm/+ ath1-5,* and *stm ath1-5* fruit in comparison to the fully fused septa of wild-type fruit, and measured the extent of the fusion defects by determining the average percent of the septa present for the fruit of each genotype.

METHODS

I. Planting and Growth Conditions

To simulate winter, *Arabidopsis* seeds require a cold treatment before germination. To reduce bacterial and fungal infection, seeds were sterilized with 70% ethanol for two minutes, then soaked in a 5% bleach 1% SDS solution for 15 minutes. Distilled and deionized water (ddH_2O) was used to wash away residual bleach from the seeds by adding and removing 500 μL of water three times. Another 500 μL of ddH_2O was added, and the seeds were placed in a 4°C refrigerator for two days. Before planting, the ddH_2O was removed, and a 0.1% agarose solution was added so that the seeds could be evenly distributed by pipetting.

The Landsberg *erecta* (Ler) ecotype of *Arabidopsis* was used as the wild type (WT) control in this experiment. For the mutant genotypes, the seed stocks planted were *stm, ath1-5,* and *stm/+ ath1-5* (see **Table 1**; Childers, 2018). Because plants with homozygous mutations in both the *STM* and *ATH1* genes are infertile, seed stocks have to be collected from plants that are homozygous for one mutation and heterozygous for the other. The *stm/+ ath1-5* seed stock is derived from parents heterozygous for the *stm* allele, meaning that one of the two alleles is mutated. Since the *STM* and *ATH1* genes are not linked, according to Mendelian genetics, approximately 25% of the seeds from the *stm/+ ath1-5* stock should have an *stm ath1-5* double mutant genotype. Eight trays were planted of the *stm/+ ath1-5* seed stock to maximize the number of plants with homozygous mutations in both genes, and two trays were planted for the each of the other

genotypes (*Ler* WT*, stm, ath1-5*), resulting in fourteen trays total (**Table 1**). Each tray contained ten pots.

Water was added to Promix BX soil (Premier Tech Horticulture, Quakertown, PA) to dampen it before adding loosely compacted soil to each pot. Each pot was labeled with its respective genotype. Using a 20 μL pipette, twenty-seven seeds were planted in a 3x3 grid-like formation with three seeds deposited into each of the nine positions. Lids were placed on the tray to provide a humid environment during seed germination and early seedling growth (2-3 weeks). Seedlings were then thinned to approximately twelve to fifteen plants per pot, and Marathon 1% granular pesticide (OHP, Inc., Mainland, PA) was added. Plants were watered Monday, Wednesday, and Friday, alternating between water with or without Miracle-Gro® Water Soluble All Purpose Plant Food (Miracle-Gro® Lawn Products, Inc., Marysville, OH) diluted to 200 ppm. Plants were exposed to 16 hours of light and 8 hours of darkness at an average temperature of 23°C with 70% humidity. Planting, thinning, and watering were carried out with the help of Kate Childers and other Liljegren lab members.

Table 1: Seed Stocks

Seed Stock Name	Number of Trays Planted	Date of Seed Collection	Possible Genotypes
Ler Wt B	1	7/9/2016	WT
sta1 #1	1	5/25/2017	*stm*
sta1sta2 #178 #2	2	10/5/2016	*stm ath1-5, stm/+ ath1-5, stm ath1-5*
sta2 #3	1	5/30/2017	*ath1*
sta1sta2 #6	2	10/12/2016	*stm ath1-5, stm/+ ath1-5, stm ath1-5*
Ler Wt B	1	10/19/2017	WT
sta1 A	1	11/23/2016	*stm*
sta2 A	1	11/23/2016	*ath1-5*
sta1sta2 #178 #2	1	10/5/2016	*stm ath1-5, stm/+ ath1-5, stm ath1-5*
sta1sta2 #6	1	10/12/2016	*stm ath1-5, stm/+ ath1-5, stm ath1-5*
sta1sta2 #178 #1	1	10/4/2016	*stm ath1-5, stm/+ ath1-5, stm ath1-5*
sta1sta2 #182 #9	1	7/5/2016	*stm ath1-5, stm/+ ath1-5, stm ath1-5*

II. Genotyping

DNA Extraction:

Genomic DNA was extracted from the leaves of mutant plants using the Plant DNeasy© Plant Mini Kit (QIAGEN, Hilden, Germany). First, tissue samples were manually disrupted with a tissue pulverizer. 400 μL of lysis Buffer AP1 was used to disrupt lipid membranes and release DNA. 4 μL of RNase A was added to each sample to breakdown RNA. All samples were then vortexed and incubated at 65°C. To neutralize the samples, 130 μL of precipitation buffer P3 was added, mixed, and incubated on ice for 5 minutes. The resulting lysate was centrifuged for five minutes at 14000 rpm and then pipetted into a Q1Ashredder spin column in a 2 mL collection tube. The lysate was centrifuged for two minutes at 14000 rpm, and the flow-through was

transferred to a new Eppendorf tube while being careful not to disrupt the pellet. For protein denaturing, 1.5 volumes of binding Buffer AW1 was added and mixed by pipetting. 650 μL of this mixture was then transferred to a DNeasy© Mini spin column placed inside a 2 mL collection tube. The mixture was centrifuged twice for one minute at 8000 rpm with the flow through liquid discarded each time. The spin column, now containing the DNA, was placed in another 2 mL collection tube. 500 μL of Buffer AW2 was then added to the samples for salt removal and purification. The mixture was centrifuged for one minute at 8000 rpm, and the flow-through was discarded. Another 500 μL of Buffer AW2 was added; this time the sample was centrifuged for two minutes at 14000 rpm. The spin column was transferred to a final 2 mL microcentrifuge tube labeled with the seed stock, plant number, and date of preparation. For elution, 100 μL of a low-salt buffer (Buffer AE) was added, and the samples incubated for five minutes at room temperature. These samples were then centrifuged for one minute at 8000 rpm. The room temperature incubation and centrifugation was repeated. The resulting plant genomic DNA was stored at -20°C and accessed when needed.

Polymerase Chain Reaction:

Polymerase Chain Reaction (PCR) is necessary to amplify the *STM* and *ATH1* gene regions using the genomic DNA obtained in the DNA extraction protocol as the template. A master mix was created using a per reaction ratio of 2 μL of 10X Standard Taq Reaction Buffer, 0.5 μL of 10 mM dNTPs, 0.7 μL of 20 mM forward and reverse primers, 0.5 μL of Taq DNA Polymerase, and 13 μL ddH_2O. To each PCR tube, 18 μL of the master mix and 2 μL of genomic DNA were added to create a 20 μL reactions for

each sample. Depending on the genotype, samples were either run on an STM-specific PCR cycle or an ATH1-specific PCR cycle in an S1000 Thermal Cycler (Bio-Rad, Hercules, CA). The sequences of the primers used are shown in **Table 2**, and the conditions of the PCR cycles are described in **Table 3**.

Table 2: Primers used for PCR amplification of targeted gene regions

Primer Name	**Sequence (5' – 3')**
ATH1-5 Forward	GGATGTTCCAAAACTTCCTTCACCC
ATH1-5 Reverse	GCTTGATTTTTTCCTAGCCCTAATCTC
STM Forward	GTTCATAAACCAGAGGAAACGGCACTG
STM Reverse	GAGGAGATGTGATCCATTGGGAAAGG

Table 3: PCR conditions for amplification of targeted gene regions

	STM		***ATH1***	
Step	**Temperature (°C)**	**Time (seconds)**	**Temperature** (°C)	**Time (seconds)**
1	94	240	94	240
2	94	30	94	30
3	55	30	54	30
4	72	30	72	30
5	Repeat steps 2-4 30 times		Repeat steps 2-4 30 times	
6	4	Forever	4	Forever

Ethanol Precipitation:

A high salt concentration in the PCR buffer can disrupt the activity of some restriction enzymes, so the *ATH1* PCR products were desalted using an ethanol precipitation. 60 μL of 100% ethanol (stored at -20°C) and 2.1 μL of 3M sodium acetate at pH 5.2 were added to the PCR product. The samples were then incubated overnight in a -20°C refrigerator. After incubation, the samples were centrifuged at 4°C and 15000 rpm for 45 minutes. Taking care not to disturb the pellet, the ethanol supernatant was

removed. To the pellet, 250 μL of 70% ethanol (stored at -20°C) was added. The sample was centrifuged again at 4°C and 15000 rpm, this time for 15 minutes. 200 μL of the ethanol supernatant was removed, then the samples were placed in a Vacufuge™ (Eppendorf, Hamburg, Germany) to evaporate the remaining ethanol from the pellet. This process takes around 20 minutes. The pellet was then resuspended in 20 μL ddH_2O prior to use of the desalted DNA in restriction enzyme digests.

Restriction Enzyme Digests:

Homozygous *stm* plants were distinguished from wild type and heterozygous *stm/+* plants using a BsrI restriction site that is only present in the wild-type allele of the *STM* PCR product. The BsrI enzyme cuts the wildtype PCR product into 106 base pairs (bp) and 29 bp fragments, while the uncut *stm* mutant PCR product remains 135 bp. The digest reaction ratio is 17 μL of the sample PCR product, 2μL of 10X NEBuffer 3.1, and 1 μL of BsrI (New England BioLabs, Ipswich, MA). The 20 μL digests were incubated for four hours at 65°C. After gel electrophoresis of the digested PCR products (see below), the genotype of the samples could be diagnosed. If the plant was homozygous for the wild type *STM* allele, only the 106 bp product appeared on the gel. If the plant was homozygous for the *STM* mutant allele, only the 135 bp product appeared; However, if the plant was heterozygous for the *STM* mutant allele, both the 135 bp product and the 106 bp product appeared.

To distinguish between homozygous *ath1-5* mutant and wild type plants, a MluCI restriction site was used because only one of two sites is present in the mutant *ath1-5* PCR product compared to the wild-type *ATH1* PCR product. PCR products were digested

using a MluCI restriction enzyme (New England BioLabs, Ipswich, MA) in the 10X CutSmart Buffer (New England BioLabs). Mutant PCR products were cut into 306 bp, 158 bp, and 115 bp fragments, while the wild type PCR product was cut into 421 bp and 158 bp fragments. These samples (3 μL master mix, 17 μL PCR) were incubated for three hours at 37°C. After gel electrophoresis, the genotypes were diagnosed as follows: if the plant was homozygous for the wild type *ATH1* allele, only the 421 bp product appeared, while only the 306 bp product appeared if the plant was homozygous for the *ATH1* mutant allele.

Gel Electrophoresis:

After completion of the digest, the genotype of each DNA sample was determined using gel electrophoresis, which separates DNA fragments by length. Agarose was dissolved into 1X TAE buffer using a microwave, and 5.5 μL of 1% ethidium bromide was added to the solution. This solution was poured into a gel mold with a comb to create the wells, and rested at room temperature until the gel was solidified. 3% agarose gels were used to separate the STM PCR products because there is a smaller difference in size between these products. The 3% gel was made with 6 g agarose, 200 mL TAE, and 5.5 μL ethidium bromide. For ATH1 PCR products, 1% agarose gels were used. These gels were made using 2 g agarose, 200 mL TAE, and 5.5 μL ethidium bromide. To each DNA sample, 3 μL of 6x loading dye was added, then 13 μL of each sample was loaded into the gel. To determine the sizes of the DNA fragments, a 50 bp ladder was used for the 3% gels, and a 1 kb ladder was used for the 1% gels. The electrophoresis was run at 100V for around 45 minutes.

Gel Imaging:

An AlphaImager HP was used to image the gels. The gels were viewed with ultraviolet (UV) light to detect the fluorescence of ethidium bromide, a chemical that intercalates with DNA fragments.

III. Fruit Data Collection

A total of 92 plants were observed for this study: 18 wild-type, 18 *stm*, 18 *ath1-5*, and 38 *stm ath1-5* plants. Three fruit from each plant were analyzed and imaged. To control for potential phenotypic differences resulting from the age of the shoot meristem when the floral meristems were initiated, fruit were selected from among the fifth to fifteenth flowers produced on the primary stem. Data were collected when the fruit had begun to turn yellow and were on the verge of dehiscence (late stage 17 of flower development; Smyth et al., 1990). This stage of development was chosen to take advantage of the natural pod-shatter mechanism that releases the carpel valves, to more easily view the septum without damaging it. Fruit were placed on a piece of double sided tape attached to a microscope slide labeled for that particular plant. The slide was then placed on a sheet of black construction paper and viewed through a Leica S6E dissecting microscope (Leica Microsystems, Wetzlar, Germany). Using a pair of forceps, fruit were gently pressed along the valve margin to release the carpel valves and view the septum. Petals and ovules were carefully brushed away with the forceps, and a millimeter ruler was positioned next to the fruit. As shown in **Figure 5**, photos of the septa were taken through the dissecting scope lens using an iPhone 7s (Apple, Cupertino, CA). The plant number, fruit position, and a description of the septum were documented for each fruit observed.

IV. Fruit Measurements

Photos of each fruit were organized by genotype and then uploaded to the NIH ImageJ software to quantitatively analyze. The image was first magnified with the zoom tool to fit the screen, and then centered with the scrolling tool. To calibrate, the millimeter ruler photographed next to each fruit was used to set the scale. With the "*Straight*" tool, one millimeter was traced on the ruler in the image, and the amount of pixels traced was set to equal one mm by selecting "analyze" from the tool bar and "set scale" from the drop down menu. The outer edge of each fruit's septum was traced using the "freehand selections" tool to determine the potential septum surface area, shown in **Figure 5A**. After each measurement, "analyze" was selected in the toolbar, and then "measure" was selected from the drop-down menu. This produced surface area measurements (in mm^2) of the area encompassed by the freehand tracing. The surface area of the holes in the septum were then measured using the same process (**Figure 5B**). Each of these measurements was taken twice for each fruit to increase accuracy.

A.

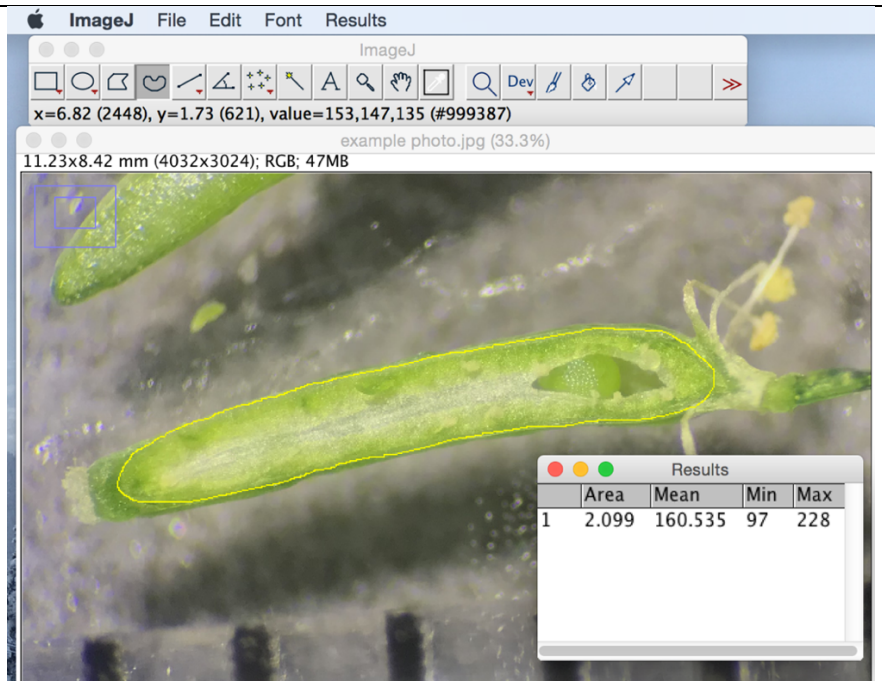

B.

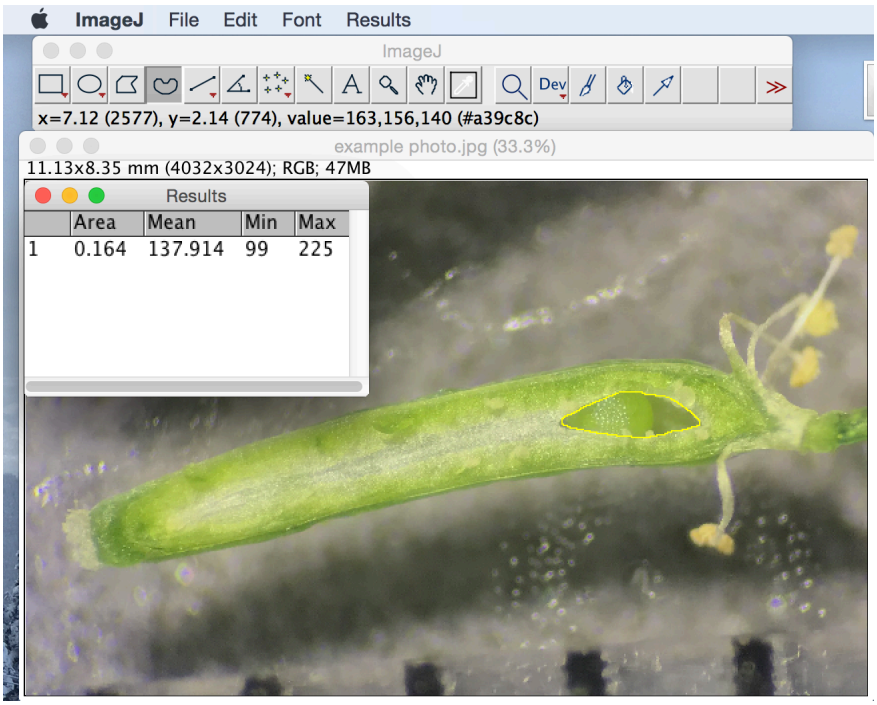

Figure 5: Procedure for determining the percentage of the septum area missing in each fruit. NIH ImageJ software was used to trace and measure **(A)** the total area of the septum and **(B)** the area of the septum that was missing for each fruit. The resulting area values (mm^2) displayed on the inset boxes were transferred into an Excel datasheet.

V. Data Analysis

From ImageJ, the data from each fruit were entered into Microsoft Excel and organized by genotype, plant number, and fruit number. This data was used with Excel to perform mass calculations and to create pie charts and bar graphs. To calculate the percentage of septum missing per fruit, the amount of surface area missing was divided by the potential septum surface area and multiplied by 100 for both trials per fruit. The two trials were then averaged together to obtain an average percentage missing per fruit. For percentage of septum surface area present calculations, the percentage of surface area missing was subtracted from 100. This was done for each fruit. To calculate the percentage of fruit with a fully developed septum, the number of fruit with a fully developed septum was divided by the total number of fruit analyzed and multiplied to 100.

RESULTS

The goal of this experiment was to analyze and quantify the phenotypic effects of mutations in *STM* and *ATH1* on septum development in *Arabidopsis thaliana* fruit. Different combinations of these gene mutations were observed (*stm*, *ath1-5*, *stm/+ ath1-5*, and *stm ath1-5)* to more clearly understand the role of each gene in septum fusion. Multiple sets of plants were analyzed over the course of two months. A total of 254 fruit were examined, as summarized in **Table 4**. Although three fruit were selected from each of the 92 plants, only 254 fruit were used rather than 276 because the delicate septum was sometimes damaged during analysis, and accurate data was therefore unable to be collected from damaged fruit.

Table 4: Sample collection from each genotype

Genotype	# Plants Sampled	# Fruit Sampled
WT	18	54
stm	18	51
ath1-5	18	49
stm/+ ath1-5	29	75
stm ath1-5	9	25
Total:	**92**	**254**

Figure 6 displays the percentage of fully developed septa per genotype. Each of the 254 fruit was characterized as either having a fully developed septum or having fusion defects and then classified by genotype. The wild-type and *ath1-5* single mutant fruit each had 100% fully developed septa whereas the *stm* single mutant only had 1 fruit (2%) with a fully developed septum. A larger percentage of *stm/+ ath1-5* fruit had fully developed septa (32%) than the *stm ath1-5* double mutant fruit (12%) (**Figure 6**).

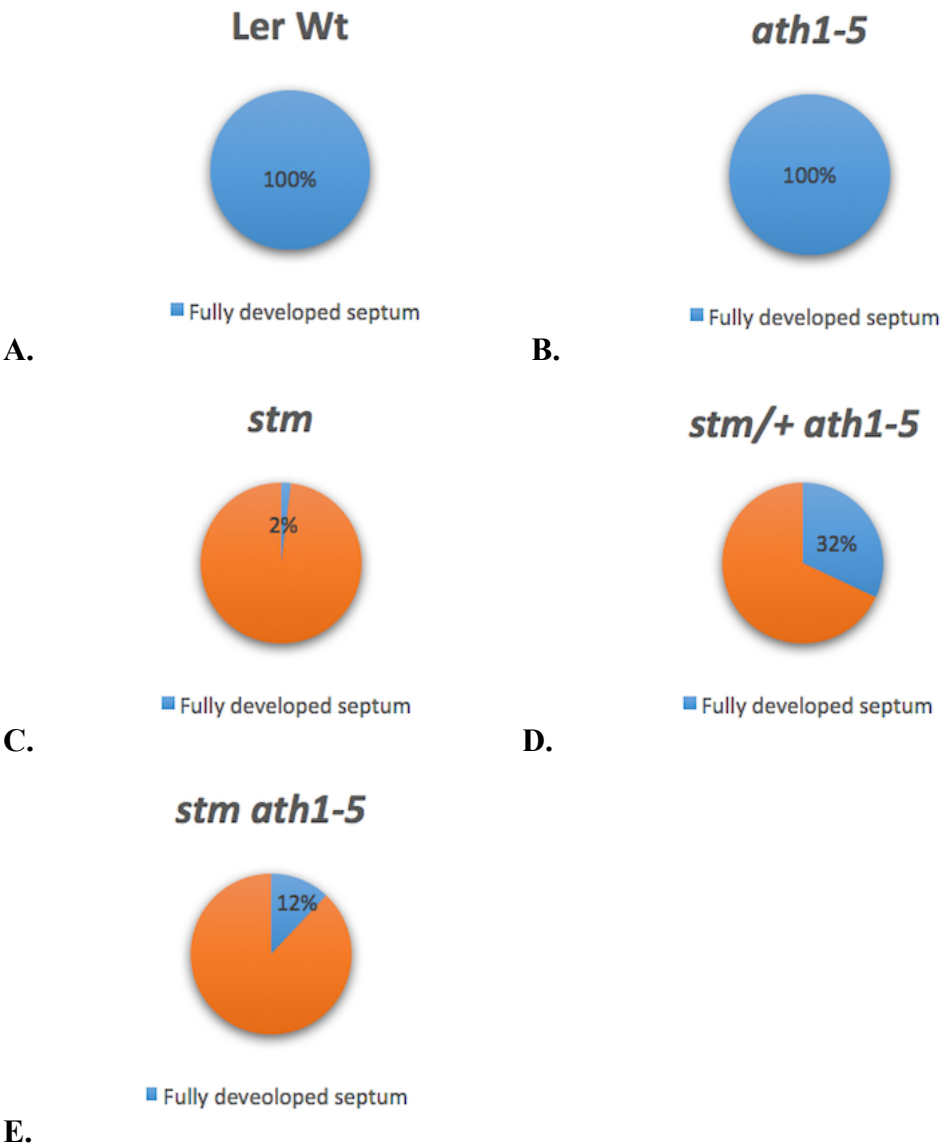

Figure 6: Percentage of fully developed septa per genotype. **A.** Each of the 54 wild type fruit analyzed had a fully developed septum. **B.** Similar to wild type, all 49 *ath1-5* fruit had fully developed septa. **C.** Of 51 *stm* fruit, only one had a fully developed septum (2%). **D.** The *stm/+ ath1-5* fruit displayed 32% fully developed septa (n=75). **E.** 12% of the *stm ath1-5* fruit (n=25) had fully developed septa.

To assess the extent of the septum defects in mutant fruit, each of the 254 fruit in this study were imaged and measurements of 1) the potential septum surface area and 2) the area of any missing part of the septum were conducted using NIH ImageJ (See

Methods). As shown in in **Figure 7**, the average potential septum surface area varied greatly between genotypes with *stm* having the smallest septa and wild type having the largest. The *ath1-5* septa were most similar in size to the wild type, while the *stm/+ ath1-5* and *stm ath1-5* septa were much smaller. The septa observed in this experiment ranged in surface area from 0.31 mm^2 to 7.5 mm^2. Due to these differences in size that reflect other developmental defects in the mutant fruit, I evaluated the extent of the septum fusion defects by determining the proportion of the septum that was missing.

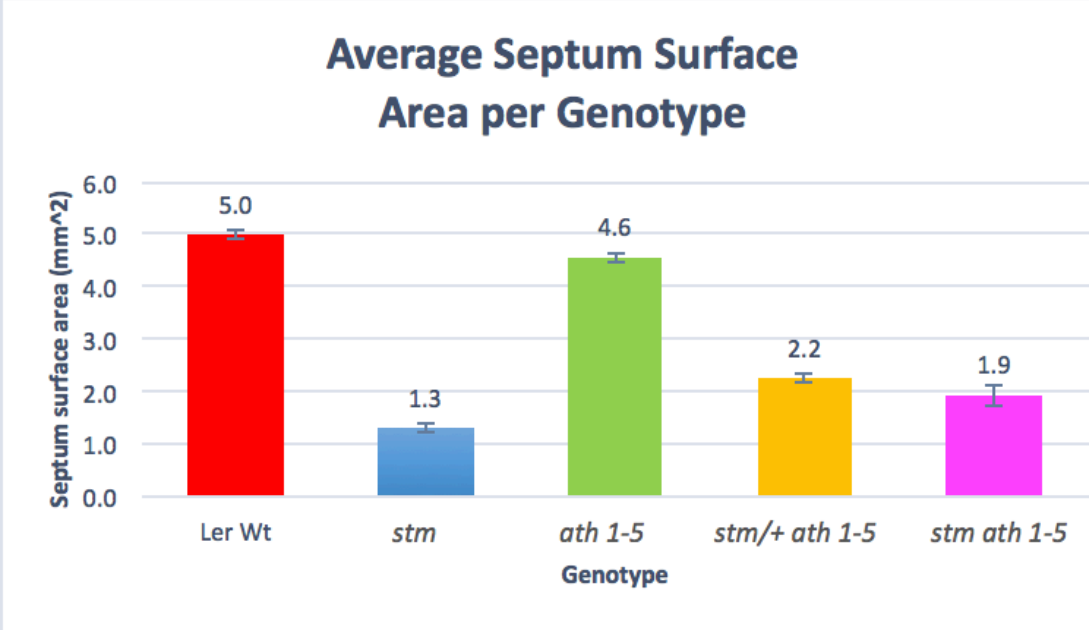

Figure 7: Average septum surface area per genotype in mm^2. The wild type fruit had, on average, a septum surface area of 5.0 mm^2. The *stm* fruit were drastically smaller than the rest with an average septum surface area of 1.3 mm^2. The *ath1-5* septa were the second largest with an average surface area of 4.6 mm^2. The *stm/+ ath1-5* septa were, on average, 2.2 mm^2, and the *stm ath1-5* septa averaged 1.9 mm^2. The standard error of the mean was 0.10 mm^2 for wild-type, 0.10 mm^2 for *stm*, 0.07 mm^2 for *ath1-5*, 0.09 mm^2 for *stm/+ ath1-5*, and 0.19 mm^2 *stm ath1-5*.

Figure 8 displays the average septum surface area missing in the fruit of each genotype studied. As discussed previously (**Figure 6**), the wild type and *ath1-5* single

mutant fruit had fully developed septa, so they were not missing any septal tissue. The *stm* single mutant and the *stm ath1-5* double mutant fruit were missing an average of 0.5 mm^2 septal tissue (**Figure 8**). The *stm/+ ath1-5* fruit were missing an average of 0.3 mm^2 septal tissue, significantly less than the *stm* and *stm ath1-5* fruit, but more than the *ath1-5* single mutant fruit.

To determine the average percentage of septum surface area present in the fruit of each genotype, the percentage of septum surface area missing was first calculated for each fruit. This was done by taking the area of the septum surface missing (**Figure 8**), dividing it by the potential septum surface area (**Figure 7**), and multiplying by 100 for each fruit. Then, to find the percentage of surface area present, the percentage of surface area missing was subtracted from 100.

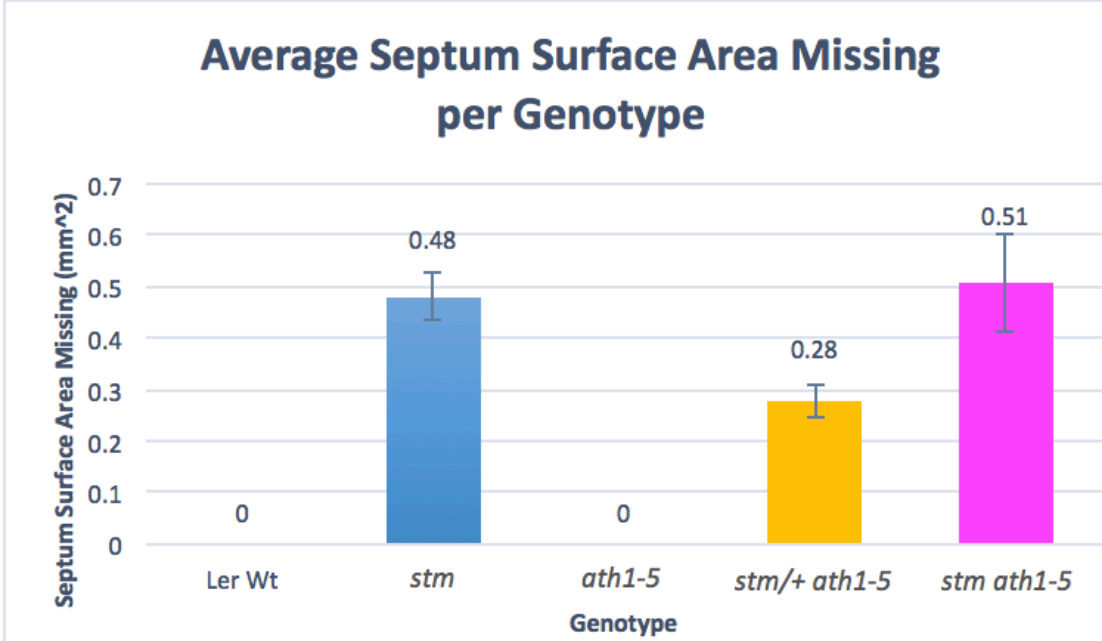

Figure 8: Average septum surface area missing per genotype. The wild-type and the *ath1-5* single mutants were not missing any septal tissue. The *stm* fruit were missing, on average, 0.48 mm^2 of their septa, and similarly, the *stm ath1-5* double mutants were missing 0.51 mm^2 on average. The *stm/+ ath1-5* were missing 0.28 mm^2 of septum surface area on average. The standard error of the mean was 0 mm^2 for wild-type, 0.05 mm^2 for *stm*, 0 mm^2 for *ath1-5*, 0.03 mm^2 for *stm/+ ath1-5*, and 0.10 mm^2 *stm ath1-5*.

Figure 9 displays the average percentage of the septum surface area present in wild-type and mutant fruit. Both *stm* and *stm ath1-5* fruit were found to be missing about 60% of their septa.

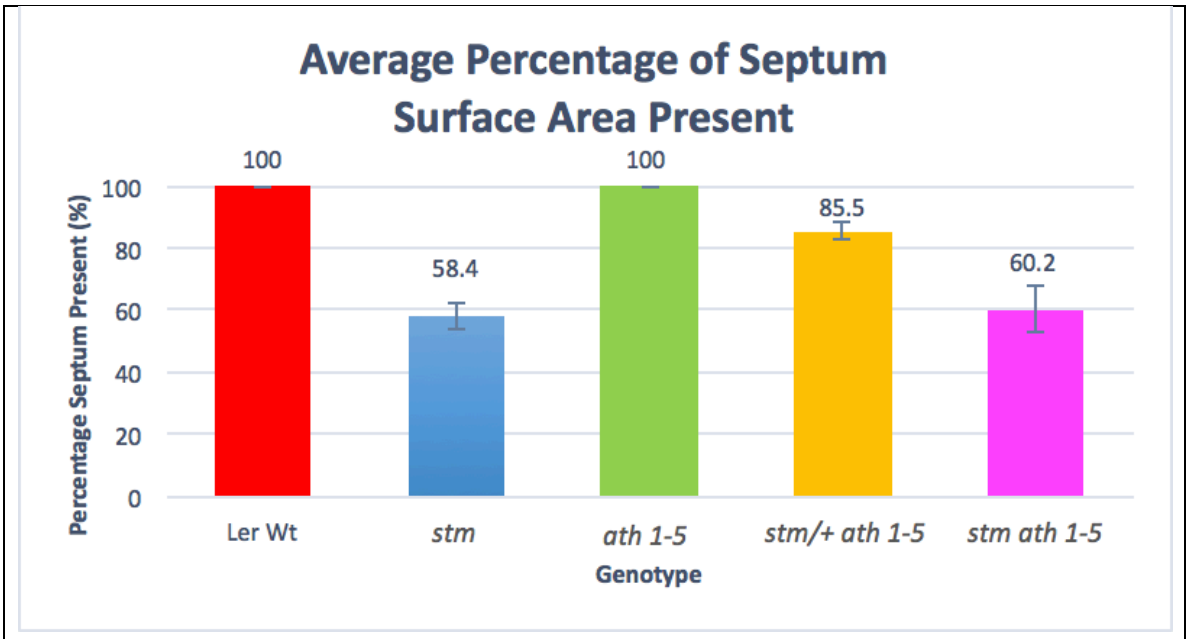

Figure 9: Average percentage of septum surface area present per genotype. Both the wild type and the *ath1-5* fruit had 100% fully developed septa. On average, only 58% of the septum was present for *stm* fruit. 86% of the septum was present for *stm/+ ath1-5* fruit, and an average of 60% of the septum was present for *stm ath1-5* fruit. The standard error of the mean 0 mm^2 for wild-type, 4.2 mm^2 for *stm*, 0 mm^2 for *ath1-5*, 2.5 mm^2 for *stm/+ ath1-5*, and 7.4 mm^2 *stm ath1-5*.

While **Figure 9** shows the average percentage of the septum present for the fruit of each genotype, **Figure 10** displays the average percentage of the septum present per plant. This analysis reveals the phenotypic diversity among *stm, stm/+ ath1-5*, and *stm ath1-5* plants and, in contrast, the consistency of complete fusion of the septum in wild type and *ath1-5* plants. For instance, while *stm* fruit had an average of 60% of their septa present, when considering individual plants, the average varied between 36 and 82% (**Figure 10**). The *stm ath1-5* double mutants showed the highest variation in septum development, with a range of 30 to 91% average septum surface area present per plant (**Figure 10**). The *stm/+ ath1-5* septa varied between 41 and 100% surface area present (**Figure 10**).

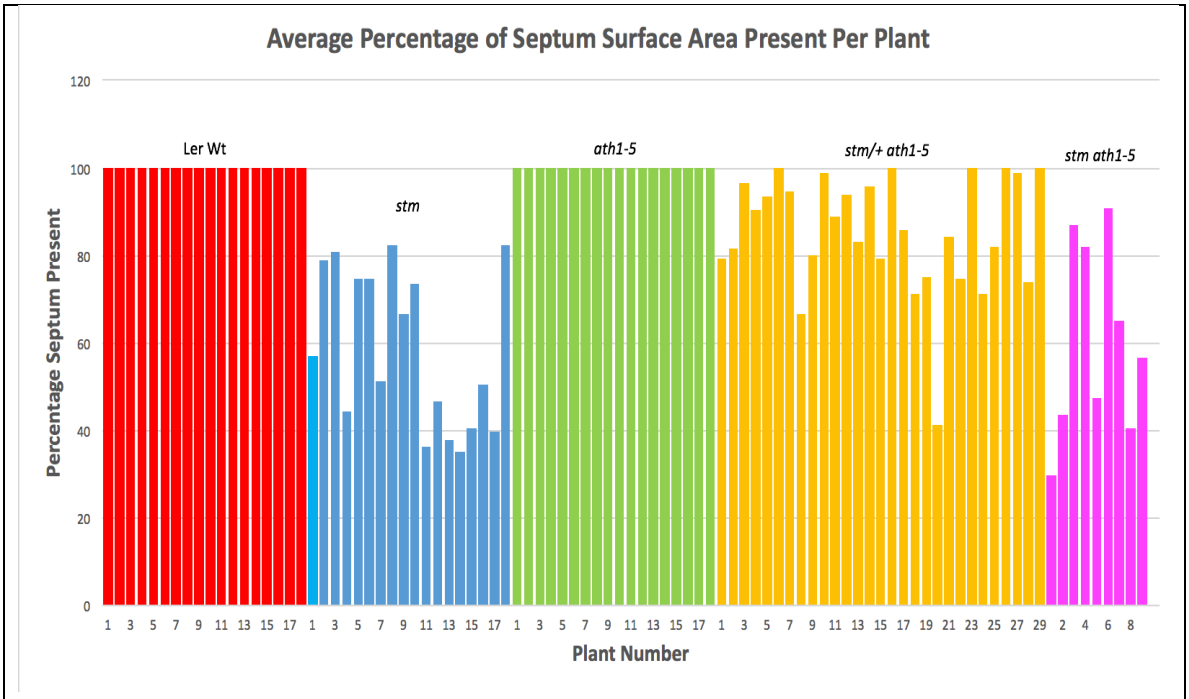

Figure 10: Average percentage of septum surface area present per plant. For the wild-type and *ath1-5* fruit, all 18 plants for each genotype had completely fused septa (100%). The amount of septum present for the *stm* fruit varied between 36 and 82%. The *stm/+ ath1-5* plants had overall a higher percentage of septum present, but varied between 41-100% percent. The *stm ath1-5* plants showed the most diversity, varying between 30% and 91%.

DISCUSSION

The goal of this experiment was to analyze the septa of *Arabidopsis thaliana* wild-type and mutant fruit to gain a better understanding of the roles of STM and ATH1 in promoting development and fusion of the septum. My first hypothesis was that the *stm* single mutant fruit would display moderate to severe septum defects due to STM's role in promoting growth of the central margin meristem via cytokinin synthesis. This hypothesis was supported by my data. Only one of the 51 *stm* single mutant fruit observed had a fully developed septa (**Figure 6**), and the *stm* septa were, on average, only 58% complete compared to the fully fused wild-type fruit (**Figure 9**). Therefore, partial loss of STM function is sufficient to interfere with growth and complete fusion of the septum.

My second hypothesis was that the *stm ath1-5* double mutant fruit would have a more severe phenotype than *stm* mutant fruit, with less of the septum present and possibly missing entirely. This hypothesis was not supported by the data. Instead the *stm* and *stm ath1-5* fruit displayed 58 and 60% of the septa present, respectively (**Figure 9**). Furthermore, my analysis of the single mutants showed that 98% of the *stm* fruit observed had septal defects, while 0% of the *ath1-5* fruit had defective septa (**Figure 6**). Taken together, these results suggest that STM plays a critical role in development of the septum, but that ATH1 does not. This finding was unexpected as previous research by Childers (2018) and Malone (2018) demonstrated that STM and ATH1 have overlapping roles in other aspects of fruit growth.

An intriguing result in my study was that *stm/+ ath1-5* fruit had septal fusion defects, with an average of 86% of the septa present. To clarify whether this was entirely due to partial loss of STM, it would be useful to directly compare wild type, *stm,* and *stm/+* fruit.

A notable observation of my study was the wide range of phenotypes observed in *stm*, *stm ath1* and *stm/+ ath1* fruit (**Figure 10**). These results suggest that there is variable expressivity of these genotypes. However, my results do not suggest that there is variable penetrance, as all of the *stm* and *stm ath1-5* plants produced fruit with septum defects. While only 25 of the 29 *stm/+ ath1-5* plants had at least one affected fruit, it is expected that if more than three fruit were examined per plant the possibility of variable penetrance would be ruled out.

In considering the experimental design of my study, one feature that could be improved is the approach to sampling *stm ath1* fruit. Since the majority of *stm ath1* flowers are completely missing a central pistil, and many flowers with a pistil do not have both valves present (Childers, 2018), the *stm ath1* fruit analyzed in my study of septum development had milder developmental phenotypes. If the *stm ath1* flowers with missing fruit (and therefore missing septa) were accounted for, a future experiment might support my second hypothesis.

A further question prompted by my study is whether STM promotes fusion of the septum throughout the gynoecium or predominantly at its base or apex. I observed that the majority of *stm* fruit with partially missing septa seemed to be the most defective toward the bottom quadrant of the fruit. To test the hypothesis that STM primarily promotes fusion of the septum at the base of the fruit, Childers (unpublished results)

performed a pilot experiment using the images of this study in which she divided each fruit crosswise into quadrants on ImageJ and scored whether or not there was a region of the septum missing for each quadrant. Her study revealed that mutant fruit were more frequently missing septa in the bottom quadrant than the top quadrant. In fact, for *stm* single mutants, *stm/+ ath1-5* heterozygous mutants, and *stm ath1-5* double mutants, there was an obvious decrease in septum defects from quadrant 4 (the basal end of the fruit) to quadrant 1 (the apical end). In the future, the surface area of septa missing in each quadrant could be measured using NIH ImageJ to fine tune this result. These preliminary results are particularly interesting because they are the opposite of what was reported for fruit carrying mutations in *SPT* (Nahar et al., 2012). In *spt* mutant fruit, the septum fusion defects were found to affect the apical end of the fruit. Further experiments investigating the interactions between STM and SPT may provide further insights into the mechanisms that regulate fusion of the septum in *Arabidopsis* fruit.

BIBLIOGRAPHY

Aida, M., T. Ishida, and M. Tasaka. "Shoot apical meristem and cotyledon formation during Arabidopsis embryogenesis: interaction among the CUP-SHAPED COTYLEDON and SHOOT MERISTEMLESS genes." *Development* 126.8 (1999): 1563-1570.

Alvarez, John, and David R. Smyth. "CRABS CLAW and SPATULA genes regulate growth and pattern formation during gynoecium development in Arabidopsis thaliana." *International journal of plant sciences* 163.1 (2002): 17-41.

Alvarez, John, and David R. Smyth. "CRABS CLAW and SPATULA, two Arabidopsis genes that control carpel development in parallel with AGAMOUS." *Development*126.11 (1999): 2377-2386.

Arabidopsis Genome Initiative. "Analysis of the genome sequence of the flowering plant Arabidopsis thaliana." *nature*408.6814 (2000): 796-815.

Arnaud, Nicolas, and Véronique Pautot. "Ring the BELL and tie the KNOX: roles for TALEs in gynoecium development." *Frontiers in plant science* 5 (2014): 93.

Childers, K. (2018). Fruit Structure in *Arabidopsis thaliana* Organ Boundary mutants. Undergraduate honors thesis, Department of Biology, University of Mississippi.

Cole, M., Nolte, C. and Werr, W. (2006). Nuclear import of the transcription factor SHOOT MERISTEMLESS depends on heterodimerization with BLH proteins expressed in discrete sub-domains of the shoot apical meristem of *Arabidopsis thaliana*. *Nucleic Acids Res.* 34, 1281-1292.

Endrizzi, K., Moussian, B., Haecker, A., Levin, J. Z. and Laux, T. (1996). The *SHOOT MERISTEMLESS* gene is required for maintenance of undifferentiated cells in

Arabidopsis shoot and floral meristems and acts at a different regulatory level than the meristem genes *WUSCHEL* and *ZWILLE*. *Plant J.* 10, 967-979.

Gomez-Mena, C. and Sablowski, R. (2008). *ARABIDOPSIS THALIANA HOMEOBOX GENE1* establishes the basal boundaries of shoot organs and controls stem growth. *Plant Cell* 20, 2059–2072.

Gubert, C. M., Christy, M. E., Ward, D. L., Groner, W. D. and Liljegren, S. J. (2014). ASYMMETRIC LEAVES1 regulates abscission zone placement in *Arabidopsis* flowers. *BMC Plant Biol.* 14,195.

Ishida, T., et al. "Involvement of CUP-SHAPED COTYLEDON Genes in Gynoecium and Ovule Development in Arabidopsis Thaliana." *Plant and Cell Physiology*, vol. 41, no. 1, 2000, pp. 60–67., doi:10.1093/pcp/41.1.60.

Larsson, Emma, Robert G. Franks, and Eva Sundberg. "Auxin and the Arabidopsis thaliana gynoecium." *Journal of experimental botany* 64.9 (2013): 2619-2627.

Leary, L. (2018). Characterizing the effects of *stm* and *ath1* mutations on floral organ development in *Arabidopsis thaliana.* Undergraduate honors thesis, Department of Biology, University of Mississippi.

Liljegren, S. J., Roeder, A. H., Kempin, S. A., Gremski, K., Ostergaard, L., Guimil, S., Reyes, D. K. and Yanofsky, M. F. (2004). Control of fruit patterning in *Arabidopsis* by INDEHISCENT. *Cell* 116, 843-853.

Liljegren, Sarah J, et al. "Control of Fruit Patterning in Arabidopsis by INDEHISCENT." *Cell*, vol. 116, no. 6, 2004, pp. 843–853., doi:10.1016/s0092-8674(04)00217-x.

Malone, H. (2018). Characterizing the effects of mutations in *STM* and *ATH1* on floral organ development in *Arabidopsis thaliana.* Undergraduate honors thesis, Department of Biology, University of Mississippi.

Meinke, D. W., Cherry, J. M., Dean C., Rounsley S. D. and Koornneef M. (1998). *Arabidopsis thaliana*: A model plant for genome analysis. *Science* 282, 662–682.

Nahar, Most. Altaf-Un, et al. "Interactions of CUP-SHAPED COTYLEDON and SPATULA Genes Control Carpel Margin Development in Arabidopsis Thaliana." *Plant and Cell Physiology*, vol. 53, no. 6, 2012, pp. 1134–1143., doi:10.1093/pcp/pcs057.

Palmer, S. (2018). Quantifying abscission defects in mutant *Arabidopsis thaliana* flowers. Undergraduate honors thesis, Department of Biology, University of Mississippi.

Reyes-Olalde, J. Irepan, et al. "The bHLH transcription factor SPATULA enables cytokinin signaling, and both activate auxin biosynthesis and transport genes at the medial domain of the gynoecium." *PLoS genetics* 13.4 (2017): e1006726.

Roth, H. (2018). The effects of mutations in the *ATH1* and *STM* genes on sepal, petal, and stamen abscission in *Arabidopsis thaliana* plants. Undergraduate honors thesis, Department of Biology, University of Mississippi.

Rutjens, B., Bao, D., van Eck-Stouten, E., Brand, M., Smeekens, S. and Proveniers, M. (2009). Shoot apical meristem function in Arabidopsis requires the combined activities of three BEL1-like homeodomain proteins. *Plant J.* 58, 641-654.

Scofield, Simon, Walter Dewitte, and James AH Murray. "The KNOX gene SHOOT MERISTEMLESS is required for the development of reproductive meristematic tissues in Arabidopsis." *The Plant Journal* 50.5 (2007): 767-781.

Scofield, S., Dewitte, W. and Murray, J.A. (2014). STM sustains stem cell function in the Arabidopsis shoot apical meristem and controls KNOX gene expression independently of the transcriptional repressor AS1. *Plant Signal Behav.* 9, e28934.

Smyth, David R., John L. Bowman, and Elliot M. Meyerowitz. "Early flower development in Arabidopsis." *The Plant Cell* 2.8 (1990): 755-767.

Steeves, T.A., and Sussex, I.M. (1989). Patterns in Plant Development (Cambridge: Cambridge University Press.)

Takada, Shinobu, et al. "The CUP-SHAPED COTYLEDON1 gene of Arabidopsis regulates shoot apical meristem formation." *Development* 128.7 (2001): 1127-1135.

Takano, Sho, et al. "gorgon, a novel missense mutation in the SHOOT MERISTEMLESS gene, impairs shoot meristem homeostasis in Arabidopsis." *Plant and cell physiology* 51.4 (2010): 621-634.